

ELASTIC-PLASTIC DYNAMIC ANALYSIS OF OPENING AREA OF AN AXIAL CRACK IN A PIPE UNDER PRESSURE

D.J. AYRES

*Engineering Science Department, Power Systems Group,
Combustion Engineering, Inc., Windsor, Connecticut 06095, U.S.A.*

SUMMARY

The manner and rate of opening of a crack in a pressurized pipe determines the rate of depressurization and the jet forces on the pipe resulting from the escape of the fluid. The jet forces and the depressurization rate are important parameters in the design of safety devices and the evaluation of margins of safety for nuclear steam supply systems.

In order to determine the greatest jet force possible, an axial crack, greater than the largest possible stable crack, is assumed to suddenly occur in the pipe under pressure. The opening area of the crack is computed by an elastic-plastic large displacement dynamic finite element analysis. This analysis is evaluated by the results of companion elastic-plastic large displacement static and elastic large displacement dynamic finite element analyses. All computations are performed on the MARC CDC general purpose finite element program.

As an example, consider the analysis of a crack 60 inches (152 cm) long in a 30 inch (76 cm) inside diameter pipe 2.5 inches (6.4 cm) thick. The pipe is under normal pressure of 2250 psi (15.5 N/mm²) when the crack suddenly appears. The opening displacement (the minor half axis of the nearly elliptical opening shape) is computed by the elastic-plastic dynamic analysis to reach a maximum value of 7.3 inches (18.6 cm) in 6 milliseconds under the assumption that no depressurization occurs. The static elastic-plastic analysis predicts an opening displacement of 3.7 inches (9.4 cm). The elastic dynamic analysis results in a maximum opening displacement of 1.1 inches (2.8 cm) in 2 milliseconds, and the corresponding elastic large displacement static analysis results in an opening displacement of 0.56 inches (1.4 cm).

The results of the analyses indicate that the opening computed by either the elastic or plastic dynamic analysis is nearly twice the opening computed by the corresponding static analysis. The ratio between the computed displacements of the elastic and plastic analyses for both the static and dynamic case is the same for this geometry and assumed material properties. This ratio, however, would be expected to not be the same for the static and dynamic cases for pipes with substantially different material properties.

Using the computed rate of crack opening, an estimate of the rate of depressurization can be made. This depressurization is then considered in order to compute a better estimate of the opening displacement. Considering that the pressure is initially at 2300 psi (15.8 N/mm²) and reaches a minimum of 1060 psi (6.9 N/mm²) in 5.7 milliseconds, the maximum opening displacement reaches 5.6 inches (14.2 cm) in 5 milliseconds. The opening area therefore for the case of depressurization is only 77% of the area computed assuming no depressurization.

These computed opening displacements and areas are in general agreement with extrapolations of the results of tests performed at Battelle Memorial Institute, (Report BMI-1908). This agreement and the logical correlation of the various types of analysis indicate that the elastic-plastic dynamic finite element analysis is an accurate tool for the computation of crack opening areas for input to the design of safety devices and the evaluation of margins of safety for nuclear steam supply systems.

1. Introduction

The design of many components of a nuclear power plant is based on the requirement that the components safely withstand the effects of severe hypothetical accidents. One such hypothetical accident is the main coolant pipe rupture. Loadings on piping supports and protective devices, fluid system internals, and subcompartment pressurization are governed by this hypothesis. One aspect of this particular hypothetical accident has been arbitrarily defined as the sudden opening of a two diameter long stationary axial crack in a straight section of either the hot leg or cold leg main coolant pipe. It is further arbitrarily assumed that the crack will open quickly to an area equal to the cross-sectional area of the pipe.

In order to determine more realistically the effects of a pipe rupture, the longest possible stationary axial crack should be determined, and the rate of opening of this crack should be computed. The prediction of the longest stationary crack in ductile piping has been attempted by both experimental and analytical means (Eiber [1] and Reynolds [2]). To date, however, it remains a difficult problem since the methods for precise quantification have not been developed. The methods for computing the opening of a given crack, however, have been developed in the form of nonlinear finite element programs.

To determine the most conservative (greatest) effluent force possible, an axial crack, greater than the largest possible stable crack, is assumed to occur suddenly in the pipe under pressure. The hypothetical two diameter long crack surely is greater than the largest possible stable crack and therefore will be used in this analysis. The opening area of the crack is computed by an elastic-plastic large displacement dynamic finite element analysis. This analysis is supported by the results of companion elastic and elastic-plastic static and dynamic analyses. All computations are performed on the MARC-CDC general purpose nonlinear finite element program [3].

2. Static Analysis

In order to evaluate the finite element mesh and to obtain some preliminary information on the nature of the crack opening phenomena, several static analyses are performed. A schematic of the cracked pipe geometry is shown in Figure 1. The pipe inside diameter is 30 inches (0.76m) and the thickness is 2.5 inches (0.064m). This pipe is similar to the cold leg of a nuclear steam supply system. The hypothetical axial crack length, $2a$, is 60 inches (1.52m).

The finite element mesh of the section of the pipe shaded in Figure 1 is shown in Figure 2 in pipe midsurface coordinates, i.e., flattened out so it can be seen more clearly. The remote boundary is constrained to have a uniform axial motion. The element used is an isoparametric curved triangular thin shell based on the Koiter-Sanders shell theory, MARC type 8. Although the mean radius-to-thickness ratio of 6.5 is great enough to suspect the thin shell assumption of ignoring transverse shear deformations, it is felt that the half crack length-to-thickness ratio of 12.0 will be a more dominant characteristic of the crack opening phenomena. The effect of this latter ratio is discussed by Sih [4].

The shell element does not contain the singularity expected at the crack tip. Because of this and the previously cited assumption of thin shell theory, the results at the crack tip are expected to be only approximate. The degree of approximation can be estimated by the results of a static elastic solution of the pipe under pressure. The stress intensity factor K_I , can be determined from the plane stress formula,

$$K_I = \frac{\delta E \sqrt{2\pi}}{4\sqrt{r}} \quad (1)$$

where δ is the in-plane opening displacement of a point (finite element node) on the crack surface at distance r from the crack tip, and E is the modulus of elasticity.

Using a value of 27.5×10^3 ksi (1.895×10^{11} Pa) for the modulus of elasticity and the normal operating pressure of 2.25 ksi (15.5×10^6 Pa), the linear elastic static analysis results in $K_I = 558$ ksi $\sqrt{\text{in}}$ (6.13×10^8 Pa $\sqrt{\text{m}}$) using the displacement the closest node (0.05a). A previous solution by Erdogan and Kibler [5] for this same case produces a value of $K_I = 667$ ksi $\sqrt{\text{in}}$ (7.33×10^8 Pa $\sqrt{\text{m}}$). This difference of 16% is the result of the absence of the appropriate crack tip singularity. Evaluating K_I by eq. (1) using the normal displacement of the node at 0.1a; results in a $K_I = 692$ ksi $\sqrt{\text{in}}$ (7.6×10^8 Pa $\sqrt{\text{m}}$). This value indicates that the solution a small distance away from the crack tip can be expected to produce reasonable results.

The elastic solution indicates, as evidenced by the very large K_I , that both plasticity and geometry change (large displacement) effects must be considered. The large value of K_I also indicates that the crack is too long to remain stationary and, if existed, would probably propagate. The half opening of the center point of the crack is computed considering linear elastic, large displacement elastic, and large displacement elastic plastic behavior, and is shown in Figure 3 as a function of pressure. The stress-strain law for the elastic plastic analysis which simulates SA516 carbon steel at 550 F (288 C) is shown in Figure 4. The shape of the crack opening is illustrated in Figure 5 for the three static cases at 2.25 ksi (15.5×10^6 Pa) pressure. The resulting entire crack opening areas for the linear elastic, large displacement elastic, and large displacement elastic plastic cases are 31.2 in² (0.02 m²), 43.6 in² (0.028 m²), and 284 in² (0.183 m²) respectively. The cross-section area of the pipe is 707 in² (0.456 m²).

The static analyses indicate that consideration of both large displacement and plasticity effects is essential for a reasonable solution to the crack opening problem. The effect of plasticity is so great that the assumptions made at the crack tip are likely to have a very small effect on the crack opening areas computed.

3. Elastic Large Displacement Dynamic Analysis

The crack opening time is an important factor in determining the forces caused by the hypothetical crack rupture. Dynamic analysis is essential in order to quantify both the opening times and associated areas. A large dis-

placement elastic dynamic analysis of the 30 in (0.76 m) inside diameter pipe is performed in order to evaluate assumed time steps and to obtain a preliminary view of the phenomena without the complexity of plasticity. All of the dynamic analyses employ the Newmark β method with $\beta = 1/4$ (Nickell [6]).

For the dynamic analysis, it is assumed that the pipe is initially uncracked and under a pressure of 2.25 ksi (15.5×10^6 Pa) and suddenly the crack appears. For this case, the pressure is assumed to remain at 2.25 ksi (15.5×10^6 Pa). The static material properties are assumed to apply to the dynamic case also. The half opening of the center point of the crack vs. time resulting from two analyses utilizing time steps of 0.000025 sec. and 0.0001 sec., respectively, is shown in Figure 6. No artificial damping (Nickell [6]) is imposed on either solution.

The analysis using the smaller time step results in a maximum displacement twice the static value for the large displacement analysis. The oscillations in the results indicate the presence of higher order vibrational modes. The results of the larger time step analysis are very smooth and produce a somewhat lower maximum opening value. The larger time step, therefore, produces a slightly damped solution. The larger time step also permits a solution with much less computer time. Since the damping implied by the larger step analysis leads to a reasonable, smooth and more economical solution, it was decided to attempt the dynamic elastic plastic analysis using the larger time step of 0.0001 sec.

The shape of the crack opening at several times during the transient for the case with time step 0.0001 sec. is shown in Figure 7. The resulting entire crack opening area vs. time is shown in Figure 8. The maximum opening area is slightly greater than twice the static value and occurs at 2.2 milliseconds after the crack begins to open.

4. Elastic Plastic Large Displacement Dynamic Analysis

The effect of plasticity is determined by repeating the analysis of the 30 in (0.76 m) inside diameter crack, assuming that the pressure remains at 2.25 ksi (15.5×10^6 Pa) even after the crack opens, and utilizing a time step of 0.0001 sec. The resulting half opening at the center point vs. time is shown in comparison to the elastic results in Figure 9. The maximum opening is nearly twice the corresponding static value and occurs at 5.7 milliseconds, much later than the peak of the elastic dynamic results.

The shape of the crack opening at several times is shown in Figure 10. The resulting entire crack opening area vs. time is compared to the elastically computed values in Figure 11. The maximum crack opening area of 541 in^2 (0.349 m^2) is 77% of the cross-sectional area of the pipe and occurs 5.7 milliseconds after the crack begins to open.

It is apparent that during the opening time the pressure in the pipe will not remain constant, but will be reduced substantially by the loss of fluid. The pressure vs. time relationship can be computed by the program CEFLASH-4A [7] if an assumed opening area vs. time relationship is input. Figure 12 shows the results of this computation assuming that a 707 in^2 (0.456 m^2) area

develops both in 7 milliseconds and in 13 milliseconds. The rate of opening computed in Figure 11 is quite consistent with a 707 in^2 (0.456 m^2) area in 7 milliseconds. In order to produce a conservative (greater) opening area, however, the higher pressure curve, based on a 13 millisecond break will be used for the evaluation of the effect of depressurization.

The half opening at the center point of the crack for the case of depressurization is compared to the case of no depressurization in Figure 13. The crack opening shape for depressurization is shown in Figure 14. The resulting entire crack area vs. time is compared to the area computed in the case of no depressurization in Figure 15.

The maximum crack opening area of 420 in^2 (0.271 m^2) is 60% of the cross-sectional area of the 30 in (0.76 m) inside diameter pipe and occurs 5.0 milliseconds after the crack begins to open.

All of the above analyses have been performed on the 30 in (0.76 m) inside diameter cold leg pipe. The large hot leg pipe has a 42 in (1.07 m) inside diameter and a thickness of 4 inches (0.1 m). Because the crack opening phenomena is essentially the same for both pipe geometries only the elastic plastic large displacement dynamic analysis considering a conservative depressurization curve will be performed for the larger pipe. The depressurization curve, assuming that a crack area equal to the cross-sectional area of the larger pipe occurs in 20 milliseconds is shown in Figure 16.

Using the pressure curve of Figure 16, and the same time step of 0.0001 sec., the half opening of the center point of the 84 in (2.13 m) long crack is computed and shown in Figure 17. The opening shapes at several times are shown in Figure 18. The resulting entire crack area vs. time is compared to the area computed for the smaller pipe in Figure 19. The maximum area of 658 in^2 (0.425 m^2) is 48% of the cross-sectional area of the pipe and occurs at 7.4 milliseconds after the crack begins to open. Also shown in Figure 19 is an estimated curve developed prior to this study, by an energy based extrapolation of the test data from Eiber [1]. The area vs. time curves for both pipe geometries are very nearly identical until the maximum areas are reached. The extrapolated curve has the same fundamental slope as the computed curve but is lagging by about 1.2 milliseconds. This lag, however, causes it to nearly pass through the computed points of maximum opening. This general agreement is both support for the acceptability of the computed results and a tribute to the extrapolator's art.

5. Conclusions

The general agreement with the extrapolations of test results and the logical correlations of the various types of analysis indicate that the elastic plastic dynamic finite element analysis, via MARC-CDC, is an acceptable and accurate tool for the computation of crack opening areas. The computed areas, assuming conservative depressurization rates were substantially less than the cross-sectional areas of the pipes, and required a significant (5 to 7 millisecond) opening time.

The very high K_I values computed by the elastic analyses, and the large

openings computed by the plastic analyses indicate that the hypothetical cracks two diameters long, are likely to propagate under the design pressure. The lateral jet force would not develop if propagation occurs and the problem changes to a different break elsewhere in the system. The areas computed are therefore large enough to determine an upper bound on the force of the escaping fluid in order to establish a more realistic pipe rupture accident design basis. Further work should continue, to determine the longest possible stable crack. This will quantify more precisely the margin of safety produced by the hypothesis of a two diameter long axial crack.

References

- [1] EIBER, R. J., et al. "Investigation of the Initiation and Extent of Ductile Pipe Rupture," Final Report, BMI 1908, Battelle Memorial Institute, June 1971.
- [2] REYNOLDS, M. B., "Reactor Primary Coolant System Rupture Study-- Task C, Fracture Mechanics," Quarterly Progress Report 12, GEAP 5637, June 1968.
- [3] MARC-CDC, Developed by MARC Analysis Research Corporation. Information available through Control Data Corporation, Minneapolis, Minnesota.
- [4] SIH, G. C., "A Review of the Three-Dimensional Stress Problem for a Cracked Plate," Int. Journal of Fracture Mechanics, 7, 39-61 (1971).
- [5] ERDOGAN, F. and KIBLER, J. J., "Cylindrical and Spherical Shells with Cracks," Int. Journal of Fracture Mechanics, 5, 229-237, (1969).
- [6] NICKELL, R. E., "Direct Integration Methods in Structural Dynamics," Journal of the Engineering Mechanics Division, ASCE, V. 99, No. EM2 (April 1973).
- [7] "CEFLASH-4A, A Fortran IV Digital Computer Program for Reactor Blowdown Analysis," CENPD-133, Combustion Engineering, Inc. (August 1974).

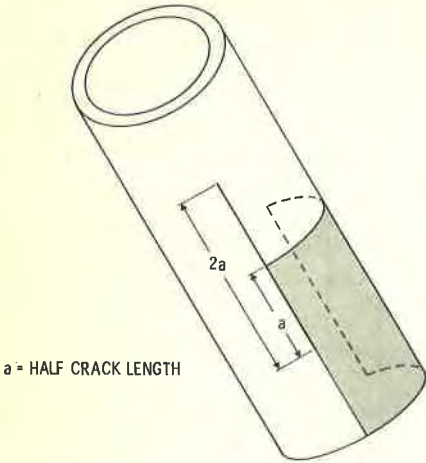


Figure 1: Geometry of pipe with hypothetical axial crack

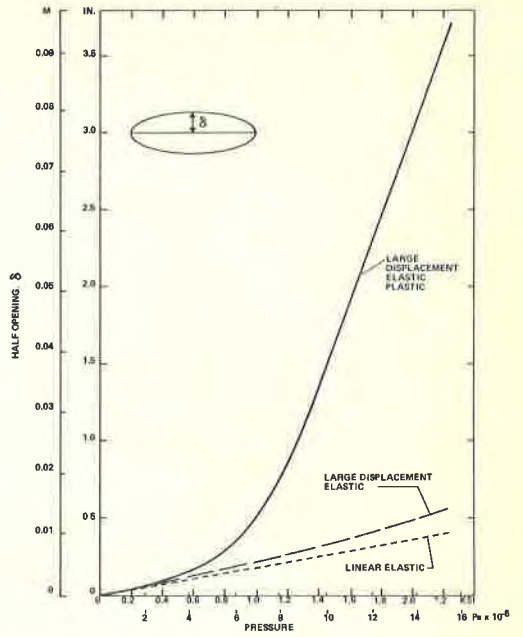


Figure 3: Half opening of center point of crack computed by static analyses

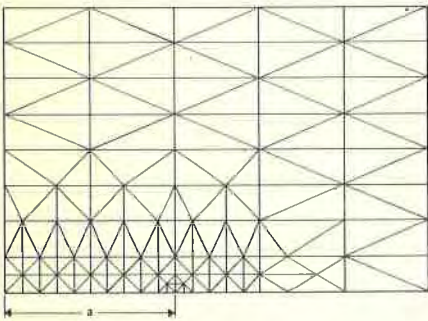


Figure 2: Finite element mesh of axial crack in pipe

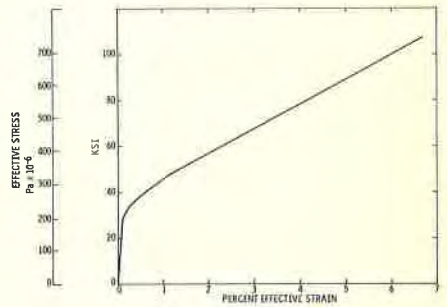


Figure 4: Effective stress strain curve for pipe material.

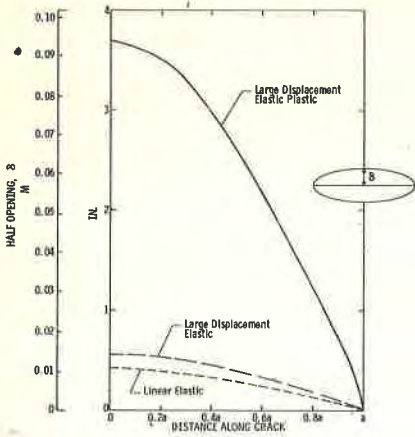


Figure 5: Opening shape of crack in 30 in (0.76 m) inside diameter pipe computed by static analyses

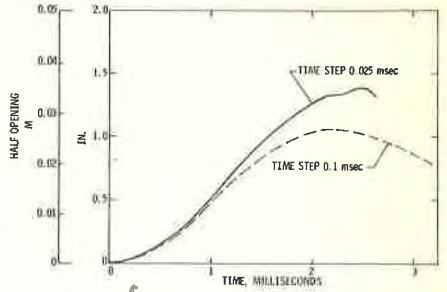


Figure 6: Opening shape of crack in 30 in (0.76 m) pipe computed by large displacement elastic dynamic analysis

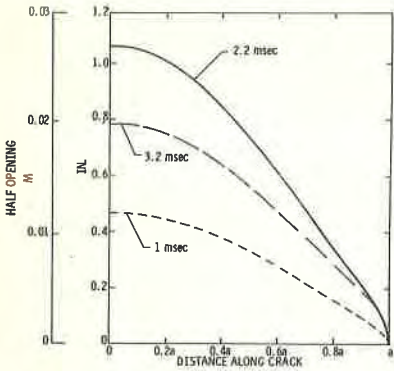


Figure 7: Half opening of center point of crack in 30 in (0.76 m) pipe computed by large displacement elastic dynamic analysis

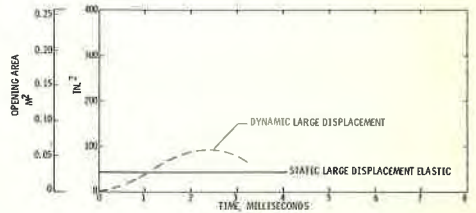


Figure 8: Opening area of crack in 30 in (0.76 m) pipe computed by large displacement elastic dynamic analysis

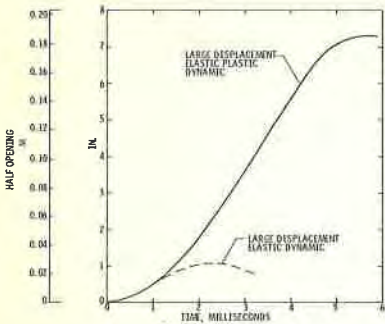


Figure 9: Half opening of center point of crack in 30 in (0.76 m) pipe with constant pressure

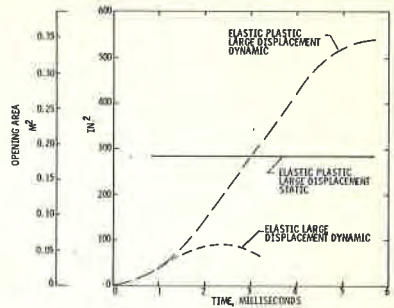


Figure 11: Opening area of crack in 30 in (0.76 m) pipe with constant pressure

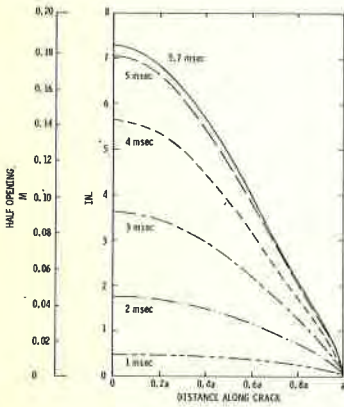


Figure 10: Opening shape of crack in 30 in (0.76 m) pipe computed by large displacement elastic plastic dynamic analysis with constant pressure

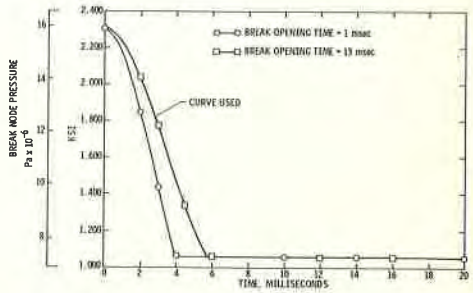


Figure 12: Depressurization of 30 in (0.76 m) pipe due to crack opening

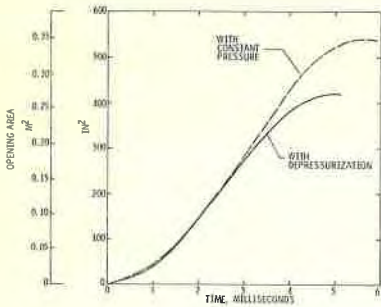


Figure 13: Half opening of center point of crack in 30 in (0.76 m) pipe computed by large displacement elastic plastic dynamic analysis

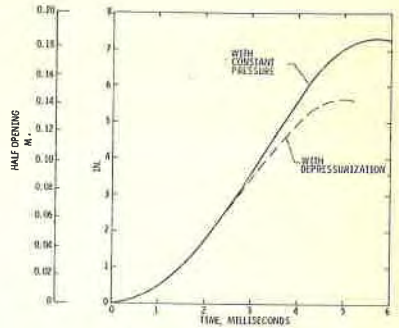


Figure 15: Opening area of crack in 30 in (0.76 m) pipe computed by large displacement elastic plastic dynamic analysis

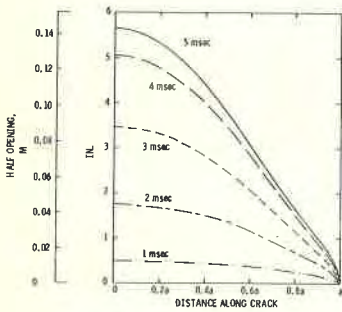


Figure 14: Opening shape of crack in 30 in (0.76 m) pipe computed by large displacement elastic plastic, dynamic analysis with depressurization

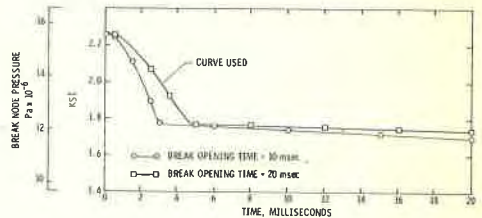


Figure 16: Depressurization of 42 in (1.07 m) pipe due to crack opening

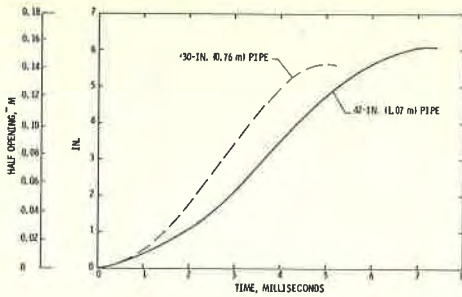


Figure 17: Half opening of center point of crack in 42 in (1.07 m) and 30 in (0.76 m) pipes computed by large displacement elastic plastic dynamic analysis with depressurization

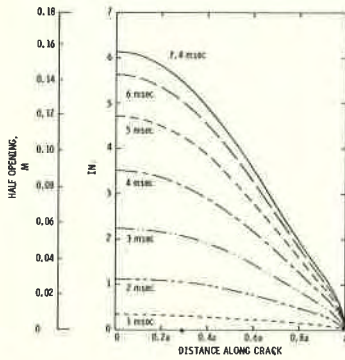


Figure 18: Opening shape of crack in 42 in (1.07 m) pipe computed by large displacement elastic plastic dynamic analysis with depressurization

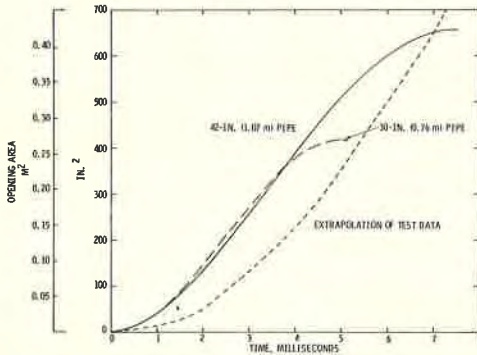


Figure 19: Opening area of crack in 30 in (0.76 m) and 42 in (1.07 m) pipes computed by large displacement elastic plastic dynamic analysis with depressurization

